

**EXPERIMENTAL INVESTIGATION OF THE LONGITUDINAL SURFACE  
STRAIN PROFILES OF PRESTRESSED NON-PRISMATIC MEMBERS**

**B. Terry Beck, PhD**, Dept. of Mechanical and Nuclear Engineering, Kansas State University

**Naga Narendra B. Bodapati**, CE Department, Kansas State University

**Aaron Robertson**, Dept. of Mechanical and Nuclear Engineering, Kansas State University

**Robert J. Peterman, PhD, PE**, Dept. of Civil Engineering, Kansas State University

**Chih-Hang John Wu, PhD**, Dept. of Industrial and Manufacturing System Engineering,  
Kansas State University

**ABSTRACT**

It is well known that the variation in cross-section and prestressing wire eccentricity of a railroad crosstie has a significant effect on the measured longitudinal surface strain profile. Resulting strain profiles for crossties depart considerably from the ideal bilinear longitudinal surface strain profile associated with a constant cross-section (prismatic) member. Departure from bilinear strain behavior presents difficulties in establishing a well-defined strain plateau region and affects transfer length assessment. This paper presents a systematic experimental investigation of the influence of cross-section and eccentricity on the resulting longitudinal surface strain profile. Several simplified non-prismatic prestressed concrete members were cast to represent a known systematic variation in cross-section shape and prestressing wire eccentricity, so as to reveal the effect on longitudinal surface strain profile variation. Measurements were made using the new multi-camera non-contact optical strain measurement system, as well as with the traditional mechanical Whittemore gauge. The unique capability of the new optical strain measurement system allows nearly continuous measurement of longitudinal surface strain. The extent to which the one-dimensional prestressed beam model can represent measured surface strain is revealed in these tests. These results have important implications in relation to the experimental measurement of transfer length for non-prismatic railroad crossties.

**Keywords:** Transfer length, railroad tie, strain measurement, pretensioned concrete

## INTRODUCTION

Knowledge of the transfer length is critical for maintaining continuous production quality in the modern manufacture of prestressed concrete railroad ties. Pretensioned concrete railroad ties are fabricated by casting concrete around already tensioned steel wires or strands. The stress transfers from the wires or strands to the concrete and is developed gradually from each end of the concrete tie, and the length required to fully develop the prestressing force is defined as the *transfer length*<sup>1,2,3</sup>. In order for the prestressing force to be fully introduced into the railroad tie at a location well before the rail load is applied, the transfer length should be shorter than the distance from the rail seat to the end of tie. In most cases, the rail seat is 21 inches from each end of the tie, but can range from 19.5 to 24 inches<sup>4</sup>.

Recent research has been focused on quantifying the parameters that affect the transfer length in pretensioned concrete railroad ties<sup>5-22</sup>. Furthermore, of critical importance to this research has been the development of a rapid non-contact optical method of assessing transfer length<sup>5,7-10,12-13,15,17-18</sup>. The goal of this work has been the practical implementation of a robust system capable of accurately measuring transfer length in the harsh in-plant environment, so that it can be used as a practical production quality control parameter.

Determination of the transfer length requires measurement of the surface strain distribution along the pretensioned concrete railroad ties. Surface strain can be measured using various mechanical, electronic (e.g., strain gauge) devices, and more recently by using optical techniques<sup>7,9,10,13</sup>. The traditional method to obtain the surface strain information is to secure metal discs called “gage points” to the surface of the specimens at 50 mm (2.0 in.) spacing prior to detensioning the strands. The distance between the gauge points is then manually measured in a slow and rather tedious process using a mechanical Whittemore gauge.

Manual measurements are simply not practical for use on a production basis in a manufacturing plant. Practical in-plant measurements of transfer length require fast and reliable surface strain measurement, along with a rapid and reliably implemented algorithm for extracting the transfer length parameter from the railroad tie strain distribution. Considerable recent progress has been made in this area, with the development of an automated Laser Speckle Imaging (LSI) transfer length measurement system<sup>7,10</sup>, and this system has been used successfully to conduct literally hundreds of in-plant crosstie measurements<sup>9,7,10,13</sup>.

Recently a more robust new type of automated multi-camera strain profiling system has been developed and successfully demonstrated in a railroad tie manufacturing plant<sup>20-21</sup>. This new system was designed as a prototype for a practical system that would not only be compatible with the tie manufacturing environment, but could be used on a production basis for quality control of tie manufacturing. The overall goal is to provide the capability of measuring the transfer length for every manufactured tie. In addition to its use for quality control, the new device, in its current portable configuration, could be used to investigate a variety of scenarios associated with the manufacture of ties, for the purpose of improving production quality. The most recent application of this instrument, prior to its use in the current paper,

was to investigate the relative significance of lubricants on pretensioning wires and strands; specifically, their effect on the wire (or strand) bond characteristics and on the important transfer length parameter<sup>21</sup>.

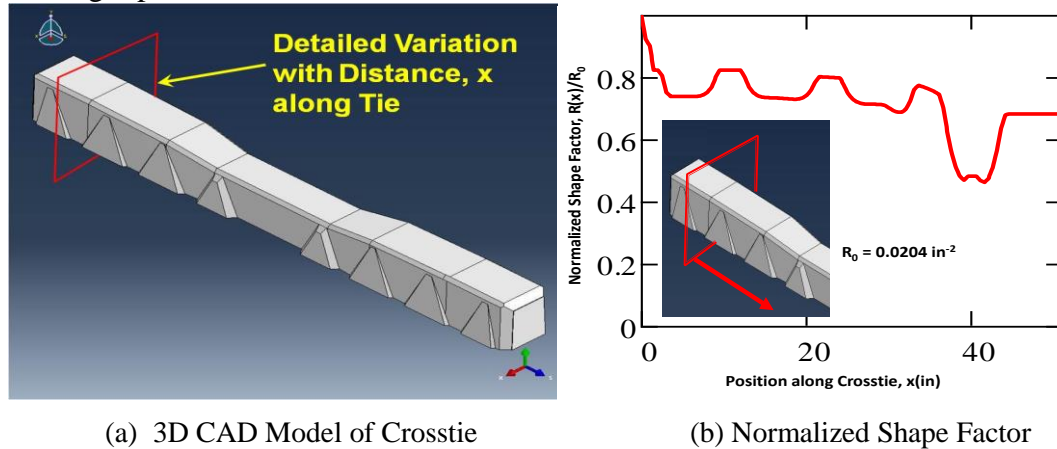


Figure 1: Typical Geometry of Concrete Railroad Crosstie

Figure 1 shows the complex geometry of a crosstie, constructed from the actual dimensions of a typical USA railroad concrete crosstie. Figure 1(a) shows the 3D (Abaqus®) model of the tie, and Figure 1(b) shows the corresponding normalized shape factor variation, which indicates the expected departures from prismatic behavior. Such strain profiles for railroad crossties can depart considerably from the ideal bilinear longitudinal surface strain profile associated with a constant cross-section (prismatic) member (e.g., a turnout tie). Departure from bilinear longitudinal strain behavior presents difficulties in establishing a well-defined strain plateau region and affects transfer length assessment. This paper presents the results of a systematic experimental investigation of the influence of cross-section and eccentricity on the resulting longitudinal surface strain profile, for the purpose of identifying the influence of key geometrical features and how well these geometrical factors can be represented by a simple one-dimensional (1D) beam bending model. The longitudinal strain under consideration is due to prestressing only, and the effects of dead load are negligible.

## DESIGN OF SIMPLIFIED NON-PRISMATIC MEMBERS

In this study, three simplified non-prismatic prestressed concrete members were cast to represent known systematic variations in cross-section shape and prestressing wire eccentricity, in an effort to reveal some of the dominant effects of shape factor on longitudinal surface strain profile variation. The intent was to depict with these simplified geometries the key (or most significant) influences of shape factor variation on the strain profile, without the increased complexity of the extremely detailed variations of shape factor suggested by the ripples shown in Figure 1(b). These ripples result from the scallops in the crosstie, which are used to reduce lateral movement of the crossties under rail loading. Also of particular interest is how well the simple 1D beam bending model used in previous analysis of transfer length assessment for non-prismatic prestressed members is capable of representing the resulting strain profiles<sup>17</sup>.

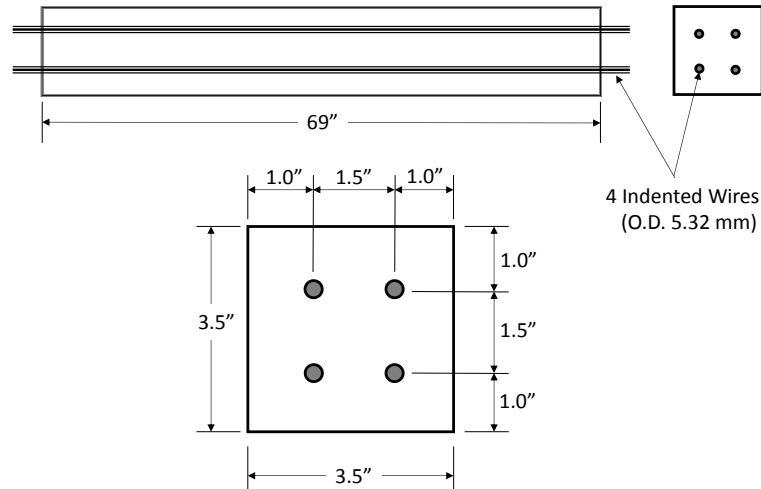
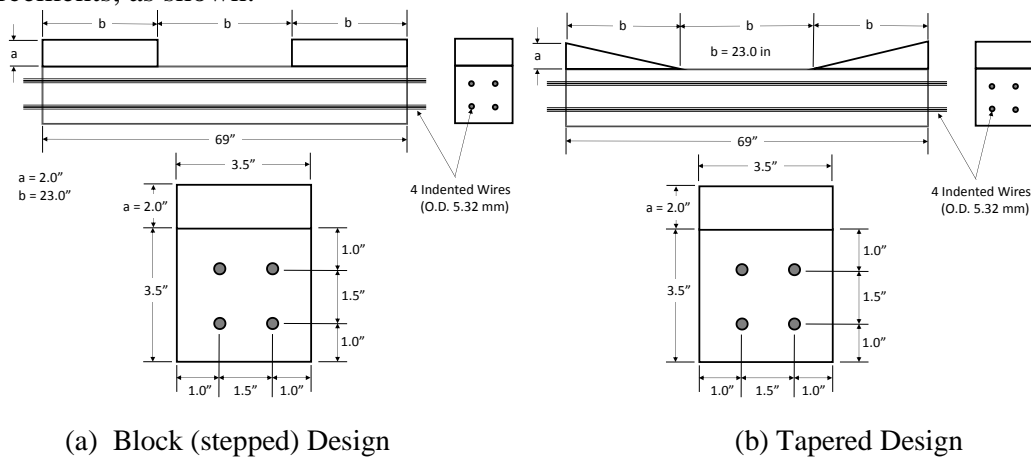


Figure 2: Baseline (control) Prismatic Prestressed Concrete Member

Figure 2 shows the geometry of a prestressed concrete prismatic member that was used as a “control” for the study. The dimensions of this member are identical to those of prisms that have been used in previous investigations of the influence of wire type on transfer length<sup>11,14</sup>. It has a fixed square cross-section with four symmetrically placed 5.32 mm indented wire reinforcements, as shown.



(a) Block (stepped) Design

(b) Tapered Design

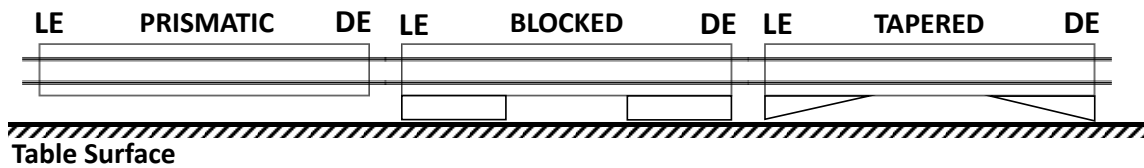
Figure 3: Non-prismatic (varying cross-section) Members

The geometries of the other two concrete members are shown in Figure 3. These members attempt to isolate and focus on two key geometrical features characteristic of the typical cross-tie shape shown in Figure 1; namely, (a) a significant reduction in cross-section in the central region of the tie, and (b) a gradual tapering of the cross-section near the end of the tie. The non-prismatic member shown in Figure 3(a) was designed to exhibit the block (or stepped) adjustment in the diameter on each end, while the non-prismatic member shown in Figure 3(b) has a gradual tapering from each end of the member toward a reduced cross-section in the middle region. The test member features are separated into three segments each having a length of 23 in (58 cm). Note that the baseline cross-section geometry is embedded within each of the non-prismatic member cross-sections shown in Figure 3; however, unlike the prismatic member, each of these designs exhibit varying cross-section

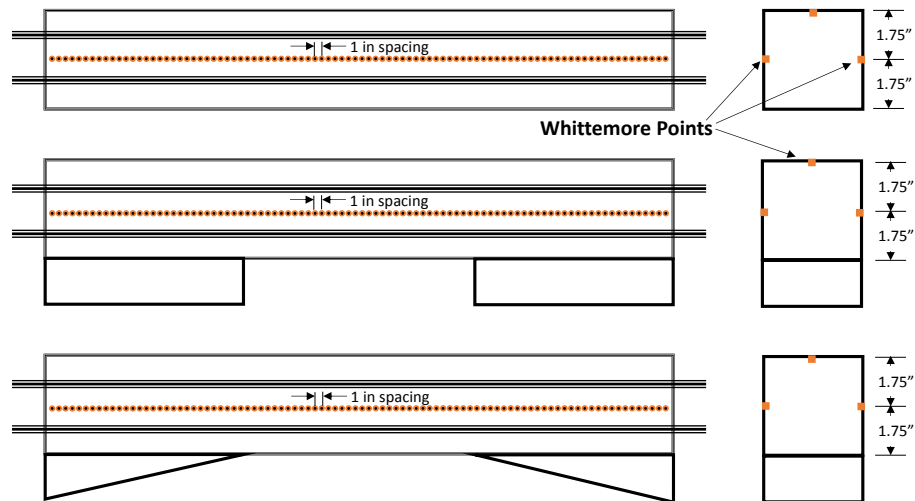
and non-uniform shape factor along their length. Hence, a significant departure from prismatic behavior is to be expected in the resulting strain profiles.

### CASTING OF PRESTRESSED CONCRETE MEMBERS

Figure 4(a) shows the layout of the inline casting of the three concrete test members described above. The live end (LE) associated with the tensioning and detensioning process is the left end of each specimen, and the dead end (DE) corresponds to the right end as shown in the Figure. Brass points were embedded as shown in Figure 4(b) on both sides of each member and also on the top surface, with a 1-in (25mm) spacing, running the entire 69 in (175 cm) span of each concrete member.



(a) In-line Casting Layout for Prestressed Concrete Test Members



(b) Layout of Embedded Whittemore Points

Figure 4: Casting of Prestressed Concrete Members and Embedded Whittemore Point Locations

Figure 5 shows a photograph of the test members aligned in the cast laboratory, with the live end on the left. Shown is the layout after tensioning and just prior to casting and subsequent detensioning. Note that the order of the in-line casting is slightly different from that depicted in Figure 4, but this order is arbitrary. A Sure-cure system was utilized to provide uniform and known concrete characteristics for the specimens. The wires were all tensioned to 7000 lbf (31 kN) each, for a total force of 28,000 lbf (125 kN). All members were cast in the upright configuration shown in Figure 4, with the flat surface on top. Concrete forms were constructed of plywood, and foam board was used to fill in the gaps beneath the members in order to maintain alignment of all top surfaces.

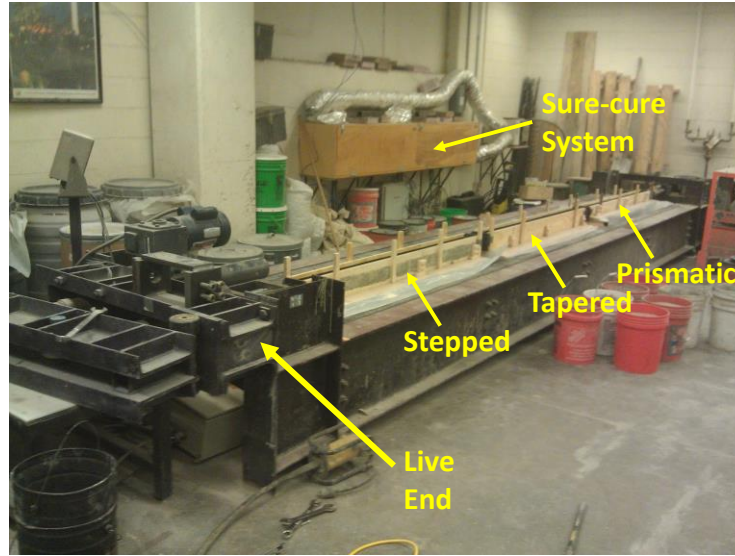


Figure 5: Photograph of Casting Bed Layout and Tensioning System

The concrete mixture used had a water-to-cement ratio of 0.32 and was similar to a mixture used by a major concrete railroad tie producer in the United States. The mixture utilized a one-inch-maximum size crushed river gravel as the coarse aggregate. The concrete was cast around 11:00 AM on April 20, 2015 and detensioning occurred approximately 13 hours later, when the concrete had reached a compressive strength of 8300 psi.

**DESCRIPTION OF STRAIN MEASUREMENTS AND TESTING CONDITIONS**

Table 1 shows a summary of the sequence of strain measurements and associated test conditions. The casting took place on Day 0, along with the initial set of surface strain measurements which first involved measurement of surface position (baseline) prior to detensioning. After detensioning, measurements of surface strain were conducted on Day 0 as well as under different environmental test conditions over the next five days.

**Table 1: Summary of Strain Measurement Testing**

DAY	TIME/DURATION	ROOM TEST CONDITION	PRISMATIC Core Temperature				STEPPED Core Temperature				TAPERED Core Temperature			
			T <sub>Le</sub> (deg F)	T <sub>MID</sub> (deg F)	T <sub>De</sub> (deg F)	AVE (deg F)	T <sub>Le</sub> (deg F)	T <sub>MID</sub> (deg F)	T <sub>De</sub> (deg F)	AVE (deg F)	T <sub>Le</sub> (deg F)	T <sub>MID</sub> (deg F)	T <sub>De</sub> (deg F)	AVE (deg F)
Day 0	8:15PM - 11:00PM	CAST, BEFORE DETENSIONING	80.1	80.7	81.7	81	84.7	82.6	84.4	84	86.2	82.9	84.4	85
Day 0	11:15PM - 3:00AM	AFTER DETENSIONING (72F)	72.8	73	73.1	73	75.3	74	74.8	75	74.8	73.5	74.0	74
Day 1	4:00PM - 8:00PM	ROOM TEMPERATURE for 24 HRS (66F)	67.2	67.2	67.2	67	67.2	67.2	67.2	67	67.2			67
Day 2	4:00PM	COLD CHAMBER SOAK for 24 HRS (40.1F)	41.4	41.4	41.4	41	41.8	41.7	41.3	42	41.1	41.7	41.8	42
Day 2	5:05PM	TEST ROOM TEMPERATURE (60.5F)	46.9	46.9	44.8	46								
Day 2	6:16PM	TEST ROOM TEMPERATURE (61.1F)					45.6	47.3	47.2	47				
Day 2	5:23PM	TEST ROOM TEMPERATURE (59.9F)									44.5	46.9	46.6	46
Day 3	4:16PM - 5:45PM	ROOM TEMPERATURE for 24 HRS (64.6F)	60.7	60.8	60.7	61	61.5	62.1	62	62	60.8	61.4	61.0	61
Day 4	4:06PM	HOT CHAMBER SOAK for 24 HRS (107.6F)	100	103.9	104.3	103	105.7	104.5	100.5	104	105.7	104.5	102.5	104
Day 4	4:49 PM	TEST ROOM TEMPERATURE (67.3F)	94.7	94	94.2	94								
Day 4	5:45 PM	TEST ROOM TEMPERATURE (67.3F)					101.1	98.5	96	99				
Day 4	5:18 PM	TEST ROOM TEMPERATURE (67.3F)									99.4	95.7	95.5	97
Day 5	4:00PM - 6:00PM	ROOM TEMPERATURE for 24 HRS (62.6F)	65.4	64.4	64.1	65	62.4	61.6	62.2	62	62.7	62.3	62.7	63

Both non-contact (optical) and traditional Whittemore gauge measurement methods were used to assess surface strain. Due to the large number of processed results that come from

the tests conducted, only a representative sample of test results will be presented in this paper. The main focus of the results presented in this paper is on the investigation of the effect of geometry on the associated strain profiles.

## COMPARISON OF MEASURED STRAIN PROFILE RESULTS

For each day of the five day testing sequence, measurements of strain were obtained for each of the geometrical configurations (PRISMATIC, STEPPED, TAPERED), using both a conventional Whittemore gauge as well as the recently developed 6-camera non-contact optical strain sensor<sup>20,21</sup>. A photograph of the entire 6-camera system in use measuring the strain profile of one of the specimens just after detensioning is shown in Figure 6(a). A close-up view of the sensor head in position above the concrete member nearest the live-end of the casting bed is shown in Figure 6(b). A simple wooden support platform was used to support the unit above the concrete surface under test, as shown. The positioning of the sensor is not critical and can be simply manually set in position before and after detensioning.



(a) 6-Camera System in Use



(b) Sensor Head and Support Platform

Figure 6: The 6-Camera Non-contact Optical Strain Sensor

The current portable version of the 6-camera system has three-point housing support and can be easily manually positioned to any desired location for measurement. It also has large depth of focus, and large lateral high resolution image capture field, so that vertical alignment and horizontal alignment are not critical. It is sufficient to simply manually mark measurement points with a felt tip marker for system positioning alignment. Realignment of the system on this felt tip marker grid is not critical and approximate manual positioning on this grid is sufficient for accurate surface strain measurement at the 5 discrete points. The nominal strain measurement accuracy is typically about  $\pm 25\text{-}50\mu\epsilon$ , which is comparable to strain measurements using the manual Whittemore gauge.

The 6-camera works by illuminating the concrete tie surface and capturing images of surface features or artificially introduced patterns that tag the surface deflection. For the current testing, microscopic reflective particles dispersed as a spray-paint were bonded to the surface and used to tag surface displacement. These images are then recorded digitally at the 6

discrete measurement points along the concrete railroad tie. An initial image set was captured before detensioning and served as a baseline image. After detensioning, a second set of images is captured, and the difference in surface deflections from these two sets of images represents the strain. For the present paper, repeated measurements were compared directly to the original baseline image obtained on day 0.

A previously developed manual shifting technique, as shown in Figure 7, was used to shift the unit in increments of 1.0 inches (25 mm) to provide increased spatial resolution over the fixed 6.0 inch (15 cm) camera spacing<sup>20-21</sup>. For the optical measurements in this paper, a single line 9-point linear shift was sufficient.

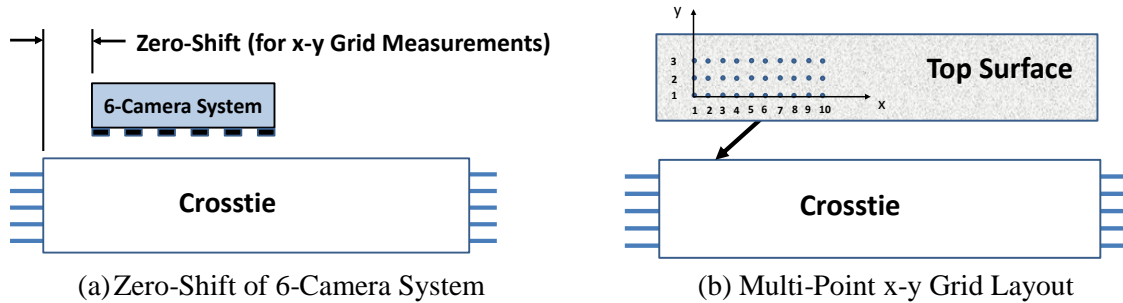


Figure 7: Zero Shifting for High-Resolution Strain Measurement

Figure 8 shows a plot of measured surface strain for the PRISMATIC member, using both optical and Whittemore gauge methods of measurement. Note that the Whittemore measurements have been subjected to a 5-point boxcar filtering process, while the optical measurements are unfiltered, and hence exhibit somewhat more random scatter.

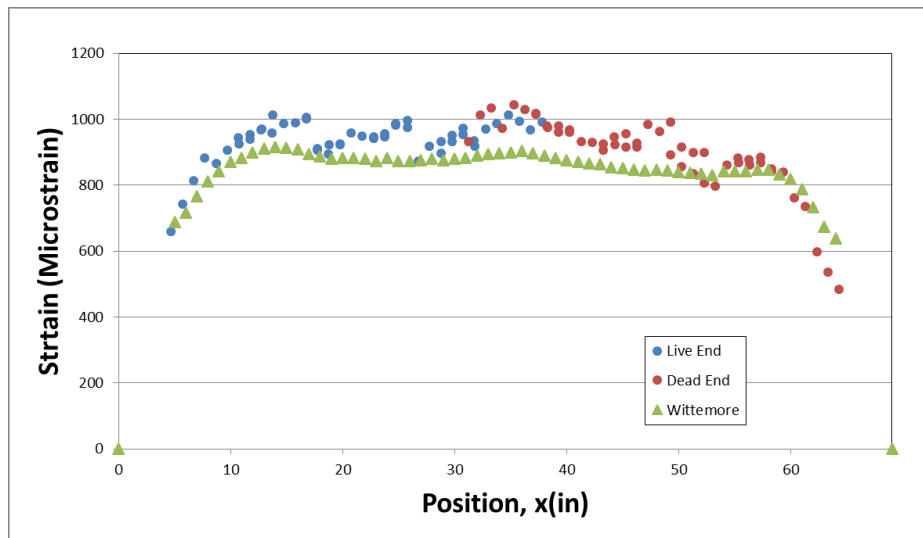


Figure 8: PRISMATIC Member Initial Strain Profile, Day 0

The results shown in Figure 8 indicate that the profile has a fairly well defined plateau which is characteristic of the strain profile for a prism. Furthermore, the optical measurements are in quite good agreement with the traditional Whittemore gauge measurements, both indicating a maximum strain level of around 900 microstrain.

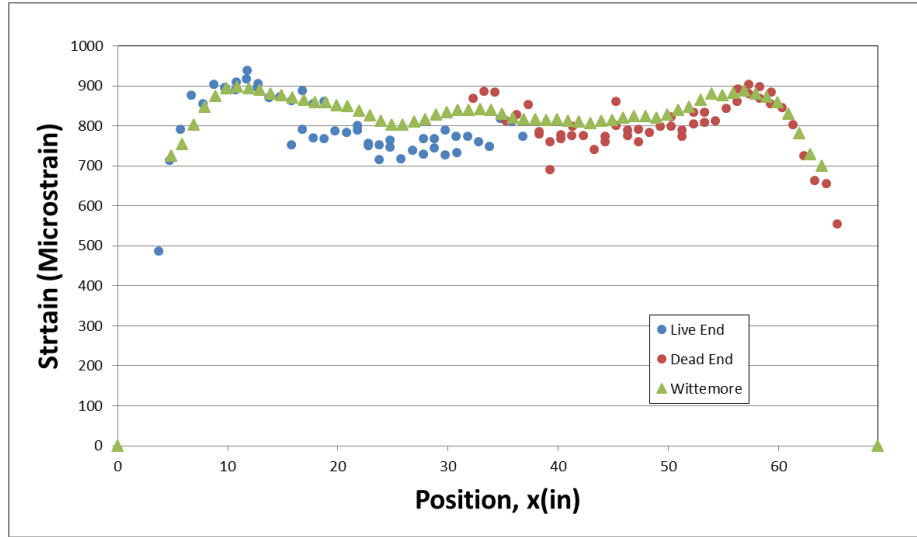


Figure 9: STEPPED Member Initial Strain Profile, Day 0

The profile in Figure 9 shows about the same maximum level of strain as the prismatic member and again the optical and Whittemore measurements are in good agreement. There is more of a dip in the strain level in the middle region in comparison to the end regions where the strain drops off rapidly. In addition, there appears to be a slight bump in the center for both prismatic and stepped members.

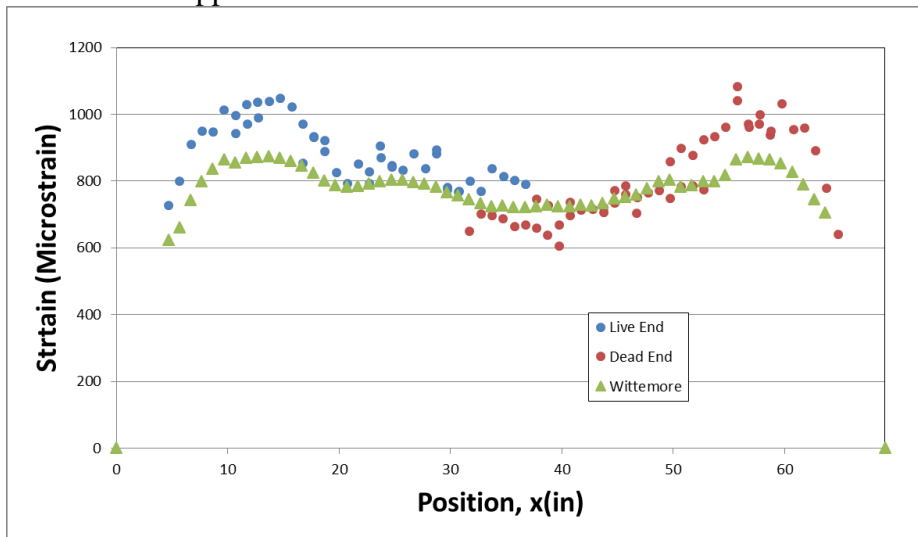


Figure 10: TAPERED Member Initial Strain Profile, Day 0

Figure 10 shows the variation of strain for the tapered member, and here a much more pronounced depression in the strain level is indicated in the middle region. Again, both optical and Whittemore measurements are in generally good agreement, although the optical measurements appear to be slightly higher near each end.

**COMPARISON WITH THEORETICAL STRAIN PROFILES**

From the known prismatic, stepped, and tapered concrete member shapes, theoretical strain profiles can be generated using the standard 1D beam bending modeling procedure. This theoretical profile shape can then also be used to arrive at a curve fit to the measured strain and at the same time determine an estimate for the important transfer length parameter.

Following the approach used in the generalized Zhao-Lee method of transfer length assessment<sup>23</sup>, the surface strain on the flat upper surface of the cast concrete members at position  $x$  (the distance that the cross-section is from the end of the member) is represented as

$$Strain(x) = \frac{P(x)}{E} \left[ \frac{1}{A(x)} + \frac{e(x)y(x)}{I(x)} \right] = \left[ \frac{P(x)}{E} \right] R(x) \quad (1)$$

where  $P(x)$  is the prestressing force or bond force at the location of  $x$ ,  $E$  is Young's modulus,  $A(x)$  is the area of the cross-section,  $e(x)$  is the eccentricity of the wire grid centroid,  $y(x)$  is the distance from the flat upper surface of the concrete member to the neutral axis of the cross-section,  $I(x)$  is the area moment of inertia of the cross-section of the concrete member at position,  $x$ , and  $R(x)$  is the so-called shape factor. Following this same analysis, it is assumed that  $P(x)$  varies linearly over the transfer length zone, from zero at the end of the pretensioned concrete member to the maximum level, and is described by

$$P(x) = \begin{cases} \frac{x}{T_L} P_{max} & x \leq T_L \\ P_{max} & x > T_L \end{cases} \quad (2)$$

where  $T_L$  is the transfer length and  $P_{max}$  is the maximum prestressing force. The determination of the transfer length is, in essence, the problem of determining the function  $P(x)$ , i.e. its parameters  $P_{max}$  and  $T_L$ , given the measured strain data points.

In addition to the determination of the key parameters  $P_{max}$  and  $T_L$ , the presence of an offset in the strain profile is generally taken into account<sup>23</sup>. This offset parameter takes into account an hypothesized (but unknown) amount of cooling of the concrete member resulting from time lapse between the baseline measurements (prior to detensioning) and those subsequent to the detensioning and cutting operation. If there is sufficient time for appreciable cooling of the concrete tie during this period, it would likely produce a type of parasitic thermal strain or offset, which is denoted by a strain offset  $TS$ . To compensate for this effect in the curve-fitting algorithm, this thermal offset parameter is introduced into the expression for the measured strain as follows:

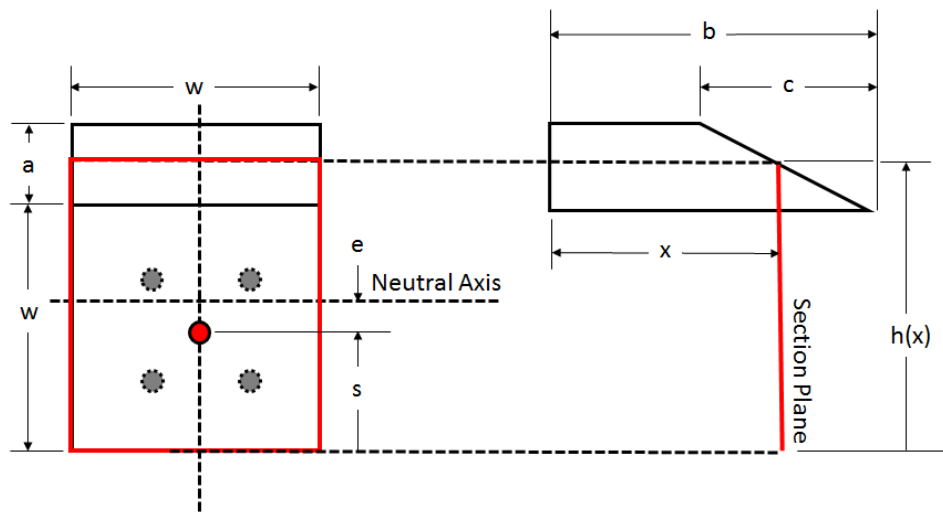
$$S_{meas}(x, P_{max}, T_L, TS) = \frac{1}{L} \int_{x-\frac{L}{2}}^{x+\frac{L}{2}} [Strain(x, P_{max}, T_L) + TS] dx \quad (3)$$

where  $TS$  is the effective thermal strain or thermally induced offset, and  $L$  is the gauge length of the strain measurement system.

Taking the random error of the strain sensor into account, the  $i$ th strain measurement value  $y_i$  at position  $x_i$  will be  $y_i = S_{meas}(x_i, P_{max}, T_L, TS) + \varepsilon_i$ , where  $\varepsilon_i$  is the random error. The random error is typically assumed to follow a normal distribution with mean zero and standard deviation  $\sigma$ ;  $i = 1 \dots N$ . The transfer length determination problem for a general non-prismatic concrete member can then be stated as follows: Given a set of data points  $(x_i, y_i), i = 1 \dots N$ , find  $P_{max}$ ,  $T_L$  and  $TS$ , so as to minimize the mean squared error (MSE) between the function  $S_{meas}(x_i, P_{max}, T_L, TS)$  and the measured  $y_i$  data. The MSE function is defined by the following:

$$MSE(P_{max}, T_L, TS) = \frac{\sum_i (S_{meas}(x_i, P_{max}, T_L, TS) - y_i)^2}{N} \quad (4)$$

Applying this general algorithm to strain measurements presented in Figures 8-10 will yield a curve fit, along with estimates of the transfer length and thermal offset parameters.

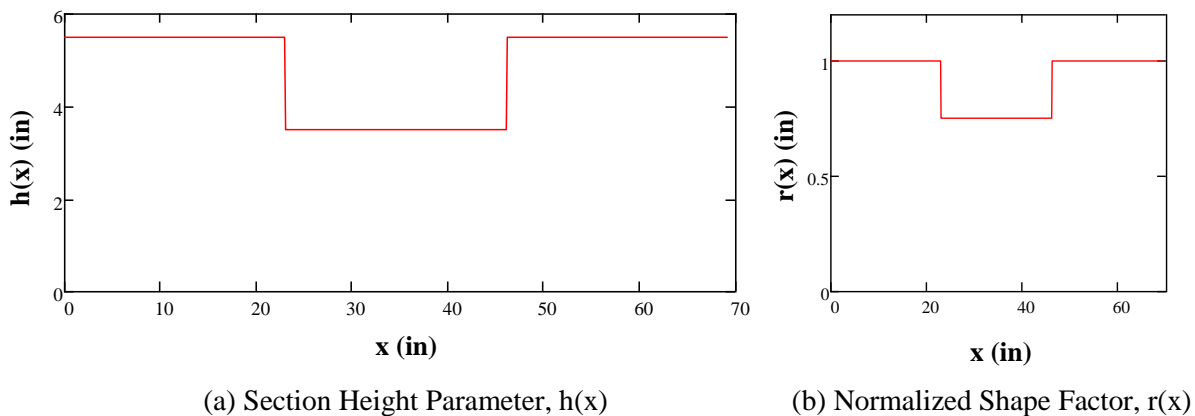


(a) End View of Non-Prismatic Member

(b) Side View of Non-Prismatic Member

Figure 11: Shape Definition for Non-Prismatic Members

The curve fitting algorithm (Modified Zhao-Lee Method) represented by Equation (5) requires an expression for the strain profile in terms of the important geometrical parameters.



(a) Section Height Parameter,  $h(x)$

(b) Normalized Shape Factor,  $r(x)$

Figure 12: Shape Characteristics for Stepped Non-Prismatic Member

A schematic diagram showing the varying cross-section for the non-prismatic members shown in Figure 3 may be represented in general by Figure 11, for the purpose of defining the geometrical parameters 1D beam bending model geometrical, and in particular, the shape factor,  $R(x)$ . The parameters  $w$ , and  $a$  are defined in Figure 3(a) and 3(b) for the stepped and tapered concrete members, and the parameter  $s$  is in all cases  $w/2$ . The variation in  $h(x)$  thus defines the profile shape of the non-prismatic members, and is shown in Figure 12 and Figure 13, along with the corresponding normalized shape factors,  $R(x)/R(0)$  for these geometries.

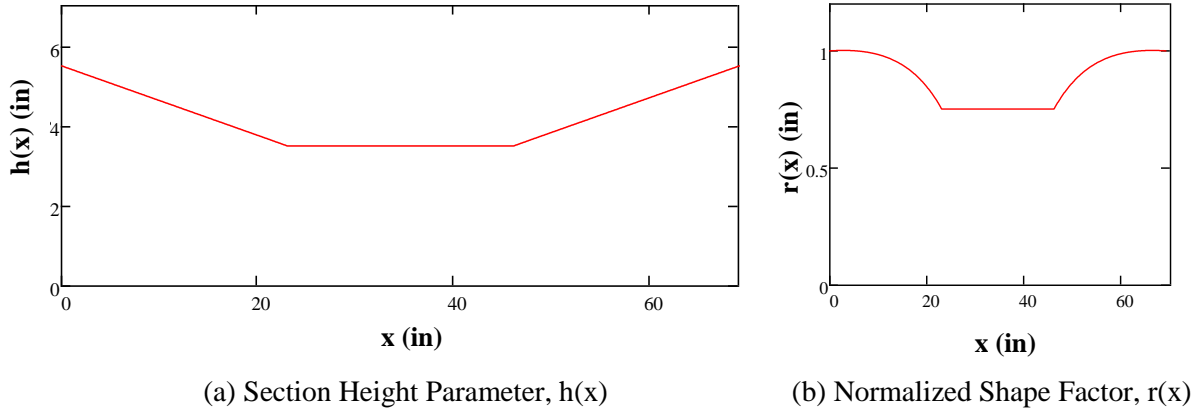


Figure 13: Shape Characteristics for Tapered Non-Prismatic Member

Using the above defined shape factor characteristics for the stepped and tapered geometries, along with the constant shape factor characteristics for the prismatic member, curve fits were conducted on the experimental strain profiles. The algorithm was applied separately to the measured strain data obtained on each end of the test members, and separate values of transfer length and thermal offset were obtained, as shown. Figure 14 gives the Whittemore measured longitudinal surface strain profiles for the prismatic member. Figure 14(a) shows the results assuming zero thermal offset, while Figure 14(b) shows the effect of including the thermal offset in the Zhao-Lee curve fitting process.

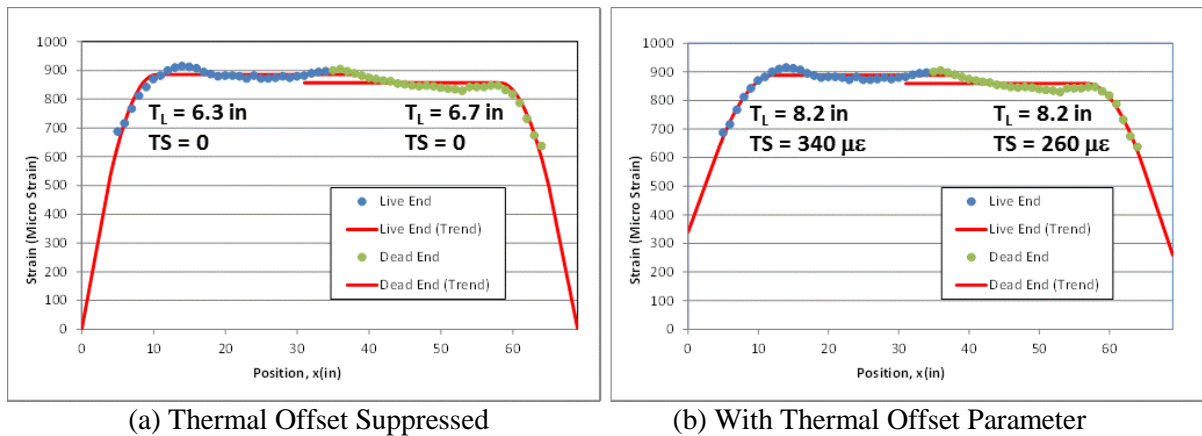
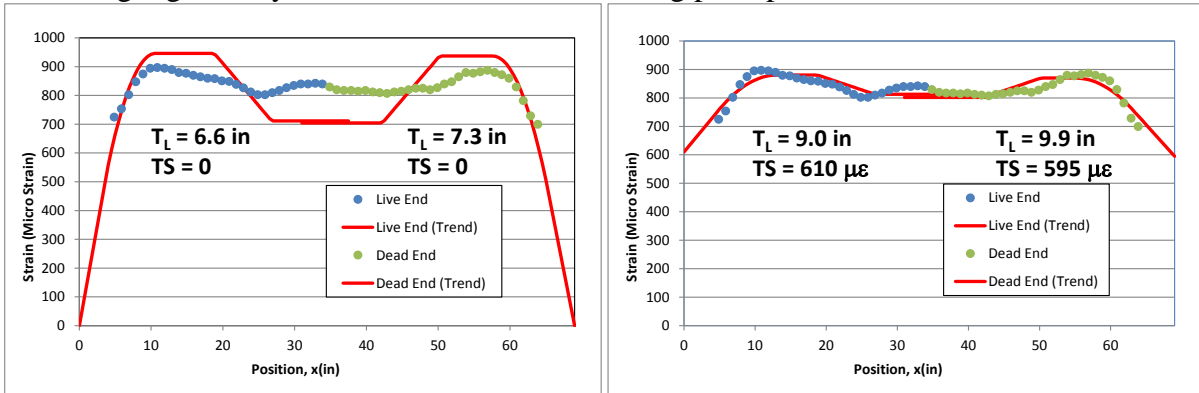


Figure 14: Prismatic Strain Profile and Transfer Length Assessment

It is apparent from a comparison between Figures 14(a) and 14(b) that a noticeable thermal offset is present, hence a somewhat larger and more representative evaluation of transfer length is achieved by accounting for this offset. The fluctuations in longitudinal surface

strain profile in the plateau region are somewhat larger than expected and may be due to a larger aggregate locally in the concrete mix, which was representative of the typical mix used in the larger geometry associated with manufacturing plant produced cross-ties.

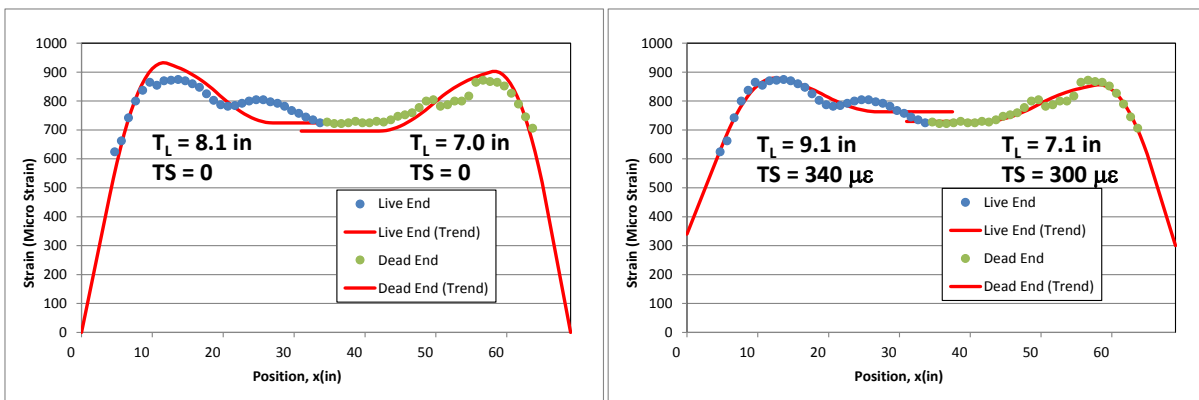


(a) Thermal Offset Suppressed

(b) With Thermal Offset Parameter

Figure 15: Stepped Member Strain Profile and Transfer Length Assessment

Figure 15 shows a comparison of measured strain profile characteristics and fitted strain profile along with transfer length assessment, for the stepped non-prismatic concrete member. Again it appears that some thermal strain should be taken into account for proper assessment of the transfer length; however, the large magnitude of the thermal strain offset is not realistic. It likely results from the fact that the 1D bending model does not appear to well-represent the strain profile resulting from the abrupt step change in cross-section. Because the strain profile doesn't capture this detail, the variation in surface strain features are smaller than expected and the curve fitting process associated with the unbiased generalized Zhao-Lee method results in a larger offset by overcompensating for this behavior. The calculated transfer length is shown to be about 2 inches higher than the assessment without accounting for thermal strain offset. If more weight is placed on the profile behavior in the developing region, it appears that the true transfer length should be closer to that for the prismatic member shown in Figure 14(b).



(a) Thermal Offset Suppressed

(b) With Thermal Offset Parameter

Figure 16: Tapered Member Strain Profile and Transfer Length Assessment

Actually, all three concrete member geometries were designed to have approximately the same transfer length. The trend shown in Figure 16 for the tapered concrete member appears to capture the detail much better than that of the abrupt stepped geometry. The assessed thermal strain offsets are also fairly reasonable, and it is clear that a better curve fit (and presumably better assessment of transfer length) results from including an offset in the transfer length assessment algorithm. However, it should be noted that the exact source of the thermal offset phenomena has never been identified experimentally, although it is suggested to be largely a thermal expansion effect.

## CONCLUSIONS

This paper has focused on the more dominant non-prismatic features associated with railroad crossties, in an effort to identify how well the simple 1D bending model can represent these features experimentally. In the efforts to establish and improve an unbiased algorithm for transfer length assessment, it is important that the potential errors in representing surface strain measurements be identified for accurate assessment of transfer length and for properly assessing transfer length uncertainty.

A first step in a systematic experimental investigation of the influence of cross-section and eccentricity on the resulting experimentally measured longitudinal surface strain profile has been presented here. Two simplified non-prismatic prestressed concrete members were cast to represent known variations in cross-section shape and prestressing wire eccentricity, so as to demonstrate the effect of the geometry on longitudinal surface strain profile variation. These two non-prismatic shapes were an abrupt stepped (or block) geometry and a tapered geometry, each of which captures one of the dominant geometrical features associated with commercially produced railroad crossties.

Measurements of surface strain were made using the traditional mechanical Whittemore gauge, as well as with the new multi-camera non-contact optical strain measurement system. The extent to which the one-dimensional (1D) prestressed beam bending model can represent measured surface strain is revealed in these tests, through comparison with the predicted behavior and through comparisons with the prismatic concrete member behavior. These results have important implications in relation to the experimental measurement of transfer length for non-prismatic railroad crossties.

The strain measurements were analyzed using the generalized Zhao-Lee transfer length algorithm, which accounted for the non-prismatic crosstie characteristics, and also compensated for the presence of thermal strain offset. The results suggest that the 1D bending model does a reasonable job in representing the tapered geometry, but has some difficulty in characterizing an abrupt change in cross-sectional area. This may suggest that the 1D strain model may have difficulties in represented accurately the more complex scalloped surface features associated with typical railroad crosstie geometry, and this may influence the reliability of transfer length assessment; particularly in the presence of an

unknown thermal strain offset. More analysis of the influence of such non-prismatic behavior on transfer length, and transfer length uncertainty in particular, is needed if transfer length is to be used eventually as a production quality control parameter. However, the results presented in this paper represent one more positive step toward an understanding of the system requirements needed for reliable in-plant automated transfer length assessment if it is to be used for in-plant quality control.

## ACKNOWLEDGMENTS

The authors would like to thank the Institute for Environmental Research (IER) at Kansas State University (KSU), under the direction of Dr. Steve Eckels, for utilization of its environmental chambers for part of the testing conducted during this research. In addition, the Department of Civil Engineering prestressed concrete casting laboratory at KSU is acknowledged for providing the facility and laboratory setup utilized in producing the prestressed concrete members. The authors would also like to thank Dr. Weixin Zhao for his assistance in making adjustments to the previously developed Zhao-Lee transfer length excel macro. The valuable assistance of Mr. Robert Schweiger, Mr. Michael Stancic, Mr. Amir Momeni, and Mr. Cale Armstrong, students in Civil Engineering, are also gratefully acknowledged for their help with casting of the concrete test specimens and with conducting the surface strain measurements presented in this paper.

## REFERENCES

1. Peterman, R. J., J. A. Ramirez, and J. Olek, "Influence of Flexure-Shear Cracking on Strand Development Length in Prestressed Concrete Members", *PCI Journal*, V. 45, No. 5, September–October 2000, pp. 76–94.
2. Gross, Shawn P., and Ned H. Burns, "Transfer and development length of 15.2mm (0.6 in.) diameter prestressing strand in high performance concrete: results of the Hobitzell-Buckner beam tests", Research report FHWA/TX-97/580-2, Center for transportation Research, The University of Texas at Austin, June 1995.
3. Kaar, P., and D. Magura., "Effect of Strand Blanketing on Performance of Pretensioned Girders", *PCI Journal*, V. 10, No. 6, December 1965, pp. 20–34.
4. Murphy, Robert L., "Determining the Transfer Length in Prestressed Concrete Railroad Ties Produced in the United States", M.S. Thesis, 2012, Kansas State University, Manhattan, Kansas, USA.
5. Wu C.-H., Zhao W., Beck T. and Peterman R. "Optical Sensor Developments for Measuring the Surface Strains in Prestressed Concrete Members" *Journal of Strains*, 47, Supp. 1, pp. 376-386, (2011), DOI: 10.1111/j.1475-1305.2009.00621.x.
6. Mark Haynes, John C.-H. Wu, B. Terry Beck, and Robert J. Peterman "Non-Contact Measurement of Wire Indent Profiles on Prestressing Reinforcement Steel" Proceedings of the 2012 AREMA Conference, Sept. 16-19, 2012, Chicago Illinois, USA.
7. Weixin Zhao, Terry Beck, Robert Peterman, John Wu, Rob Murphy and John Bloomfield, Grace Lee. "An Automated Transfer Length Measurement System for use on Concrete Railroad Ties," The 2012 PCI Convention and National Bridge Conference, September 29 - October 3, 2012.

8. Weixin Zhao ; B. Terry Beck ; Robert J. Peterman and Chih-Hang J. Wu, "A Portable Modular Optical Sensor Capable of Measuring Complex Multi-Axis Strain Fields", *Proceedings of the SPIE* 8466, Instrumentation, Metrology, and Standards for Nanomanufacturing, Optics, and Semiconductors VI, 84660Q (October 11, 2012); doi:10.1117/12.929931.
9. Weixin Zhao, Kyle Larsan Robert J. Peterman, B. Terry Beck, and C.-H. John Wu, "Development of a laser-speckle imaging device to determine the transfer length in pretensioned concrete members" *PCI Journal* Winter 2012, pp. 135-143.
10. Weixin Zhao, Robert L Murphy, Robert J Peterman, B. Terry Beck, Chih-Hang John Wu, Pelle Duong, "A Non-Contact Inspection Method to Determine the Transfer Length in Pretensioned Concrete Railroad Ties," *ASCE, Journal of Engineering Mechanics, Journal of Engineering Mechanics*, Volume: 139, Issue: 3, March 2013, pp. 256- 263.
11. Naga N.B. Bodapati, Weixin Zhao, Robert J. Peterman, John C.-H. Wu, B. Terry Beck, Mark Haynes and Joseph R. Holste, "Influence Of Indented Wire Geometry and Concrete Parameters on the Transfer Length in Prestressed Concrete Crossties," *Proceedings of the 2013 Joint Rail Conference, JRC2013-2463* April 15-18, 2013, Knoxville, Tennessee, USA. doi: 10.1115/JRC2013-2463
12. Weixin Zhao, B. Terry Beck, Robert J. Peterman, and John C.-H. Wu, "Development Of A 5-Camera Transfer Length Measurement System For Real-Time Monitoring Of Railroad Crosstie Production," *Proceedings of the 2013 Joint Rail Conference, JRC2013-2468* April 15-18, 2013, Knoxville, Tennessee, USA. doi: 10.1115/JRC2013-2468.
13. Weixin Zhao, B. Terry Beck, Robert J. Peterman, Robert Murphy, John C.-H. Wu, and Grace Lee, "A Direct Comparison Of The Traditional Method And A New Approach In Determining 220 Transfer Lengths In Prestressed Concrete Railroad Ties," *Proceedings of the 2013 Joint Rail Conference, JRC2013-2469* April 15-18, 2013, Knoxville, Tennessee, USA. doi: 10.1115/JRC2013-2469.
14. Naga Bodapati, R.J. Peterman, W. Zhao, T. Beck, C.-H. Wu, J. Holste, M. Arnold, R. Benteman, R. Schweiger, "Transfer-Length Measurements On Concrete Railroad Ties Fabricated With 15 Different Prestressing Reinforcements," *2013 PCI Convention and National Bridge Conference, September 21 – 24 at the Gaylord Texan Resort in Grapevine, Texas.*
15. Weixin Zhao, B. Terry Beck, Robert J. Peterman, John C.-H. Wu, Grace Lee, and Naga N.B. Bodapati, "Determining Transfer Length In Pretensioned Concrete Railroad Ties: Is Anew Evaluation Method Needed?" *Proceedings of the 2013 ASME Rail Transportation Division Fall Technical Conference, RTDF2013-4727* October 15-17, 2013, Altoona, Pennsylvania, USA.
16. Naga N.B. Bodapati, Weixin Zhao, Robert J. Peterman, John C.-H. Wu, B. Terry Beck, Mark Haynes and Joseph R. Holste, "Effect of Concrete Properties on Transfer Lengths in Concrete Rail-Road Ties," *Proceedings of the 2014 Joint Rail Conference, JRC2014-3859* April 2-4, 2014, Colorado Springs, Colorado, USA.
17. Weixin Zhao, B. Terry Beck, Robert J. Peterman, John C.-H. Wu, Naga N.B. Bodapati, and Grace Lee, "Reliable Transfer Length Assessment For Real-Time Monitoring Of Railroad Crosstie Production," *Proceedings of the 2014 Joint Rail Conference, JRC2014-3830* April 2-4, 2014, Colorado Springs, Colorado, USA.

18. B. Terry Beck, Weixin Zhao, Robert J. Peterman, Chih-Hang John Wu, Joseph Holste, Naga Narendra B. Bodapati, Grace Lee, "Effect Of Surface-Strain Sampling Interval On The Reliability Of Pretensioned Concrete Railroad Tie Transfer Length Measurements," 2014 PCI Convention and National Bridge Conference, September 21 - 24 at the Gaylord National Resort in Washington, D.C.
19. Naga Narendra B. Bodapati, Robert J. Peterman, Weixin Zhao, B. Terry Beck, PhD, Chih-Hang John Wu, Joseph R. Holste, Matthew L. Arnold, Ryan Benteman, Robert Schweiger, "Long-Term Transfer-Length Measurements On Pretensioned Concrete Rail Road Ties," 2014 PCI Convention and National Bridge Conference, September 21 - 24 at the Gaylord National Resort in Washington, D.C.
20. Beck, B. Terry, Peterman, Robert J., Wu, Chih-Hang (John), and Bodapati, Naga Narendra B., "In-Plant Testing of a New Multi-Camera Transfer Length Measurement System for Monitoring Quality Control of Railroad Crosstie Production," Proceedings of the 2015 Joint Rail conference, March 23-26, 2015, San Jose, CA, USA.
21. B. Terry Beck, Robert J. Peterman, John C.-H. Wu, Steve Mattson, "Experimental Investigation of the Influence of Surface Contaminants on the Transfer Length of Smooth and Indented Prestressing Reinforcements Used in the Manufacture of Concrete Railroad Ties, Paper Number: JRC2015-5751, Proceedings of the 2015 Joint Rail Conference, San Jose, CA, March 23-26, 2015.
22. B. Terry Beck, Naga Narendra B. Bodapati, Robert J. Peterman, Amir Farid Momeni, Chih-Hang John Wu, "Transfer length Measurements in Pretensioned Concrete Railroad Ties Under Rail Loads," Paper Number: JRC2015-5690, Proceedings of the 2015 Joint Rail Conference, San Jose, CA, March 23-26, 2015.